Bull. Mater. Sci. (2021)44:44
https://doi.org/10.1007/s12034-020-02334-w

Van der Waals interactions and oscillatory behaviour of carbon onions interacting with a fully constrained graphene sheet

F SADEGHI[1,2,*] and R ANSARI[3]

[1]Department of Engineering Sciences, Faculty of Advanced Technologies, University of Mohaghegh Ardabili, Namin 56199-11367, Iran

[2]Department of Engineering Sciences, Faculty of Advanced Technologies, Sabalan University of Advanced Technologies (SUAT), Namin, Iran

[3]Faculty of Mechanical Engineering, University of Guilan, P.O. Box 3756, Rasht 4199613776, Iran

*Author for correspondence (f.sadeghi@uma.ac.ir)

MS received 28 June 2020; accepted 25 September 2020

Abstract. This study focuses on the van der Waals (vdW) interactions and oscillatory behaviour of nested spherical fullerenes (carbon onions) in the vicinity of a single-layer graphene (SLG) sheet. The carbon onions are of I_h symmetries and the graphene sheet is modelled as a fully constrained flat surface. Employing the continuum approximation along with the 6–12 Lennard-Jones (LJ) potential function, explicit analytical expressions are determined to calculate the vdW potential energy and interaction force. The equation of motion is solved numerically based on the actual force distribution to attain the displacement and velocity of the carbon onion. Using the conservation of mechanical energy principle, a semi-analytical expression is also derived to accurately evaluate the oscillation frequency. Numerical results are presented to examine the influences of size of carbon onion and initial conditions (initial separation distance and initial velocity) on the operating frequency of carbon onion–SLG sheet oscillators. It is shown that carbon onion executes oscillatory motion above the graphene sheet with frequencies in the gigahertz (GHz) range. It is further observed that smaller structures of carbon onions produce greater frequencies. We comment that the presented results in this study would contribute to the development of new generation of nano-oscillators.

Keywords. Carbon onion; graphene sheet; van der Waals interactions; oscillation frequency.

1. Introduction

Over the past decades, nanoscaled materials such as graphene, carbon nanotubes (CNTs), C_{60} fullerene, carbon onions, nanopeapods and carbon nanocones (CNCs) have drawn tremendous attention from scientific communities. This is mainly due to their unique and unparalleled physicochemical properties that make them as main components for fabricating a wide range of nanoelectromechanical systems [1,2]. One of the potential applications of nanoscopic materials that has been recently the subject of numerous investigations is the creation of nanomechanical oscillators producing frequencies in the gigahertz (GHz) range or beyond [3]. Such high-frequency nano-oscillators have been proposed for use in ultrafast optical filters, nanoantennae, ultrasensitive mass detection and nonvolatile memory devices [4–7].

Nano-scale oscillators were pioneered by Cumings and Zettl [8] who experimentally observed that if the inner tube of a multi-walled carbon nanotube (MWCNT) is pulled out and released, it quickly and fully pulls back into the outer tube. They reported that the van der Waals (vdW) interaction force acting on the extruded core is the main cause of its retraction. In consistent with their experimental findings, Zheng *et al* [9] exhibited that the effect of frictional forces on the oscillation frequency of CNT oscillators is negligibly small. What Cumings and Zettl [8] observed in their experiment made it feasible to create CNT oscillators with operating frequencies up to several GHz [10,11]. Performing molecular dynamics (MD) simulations, Legoas *et al* [12] and Rivera *et al* [13] also affirmed the GHz frequency of such nano-oscillators. It was shown that stable oscillatory motion is achievable when the interwall spacing between the nanotubes is almost 3.4 Å [14]. The MD simulations were also extensively adopted to explore the mechanical energy dissipation between two contacting parties, which slide with respect to each other [10,15]. This energy causes damping in translational oscillations of oscillatory systems and is indeed an obstacle for sustained oscillations. For MWCNT oscillators, Guo *et al* [16] demonstrated that the commensuration and relative morphology of the bitube are the two key factors that affect the rate of energy dissipation. Furthermore, Zhao *et al* [17] using the chemistry at Harvard macromolecular mechanics

Published online: 18 February 2021

(CHARMM) force field method reported that frictional forces in CNT oscillators vary from 10^{-17} to 10^{-14} N per atom for various dissipative mechanisms. The capability of MWCNT oscillators in achieving high frequencies stimulated the interest of researchers to create new configurations of nanoscale oscillators. Up to now, various types of such nano-devices have been proposed, which include but not limited to C_{60} fullerene–CNT [18], CNC–CNT [19], C_{60} fullerene–CNC [20], nanotori molecule–CNT [21], ellipsoidal fullerenes–CNT [22], CNT–CNT bundle [23] and C_{60}-graphene nanoribbon trench [24] oscillators.

In recent years, nanoelectromechanical system devices constructed from graphene sheets have attracted significant attention from the research community [25]. Graphene is a monolayer of carbon atoms firmly bound in a hexagonal honeycomb lattice [26]. This novel two-dimensional (2D) nanostructure is an allotrope of carbon, which is comprised of sp^2-bonded carbon atoms with a molecular bond length of 0.142 nanometres [27]. The current interest in graphene can be attributed to its exceptional properties, such as high surface area, ultralow mass density, tunable bandgap, excellent electrical conductivity, extremely high electron mobility and strong mechanical strength [28–30]. These intrinsic properties make graphene and its related derivatives as promising candidates for a broad range of technological and scientific applications, including composite materials [31], energy storage (super-capacitors, batteries, fuel cells, solar cells) [32,33], nanoelectronics [34], catalysis [35], biosensors [36] and drug/gene delivery [37].

Since the discovery of graphene in 2004 [38], considerable efforts have been made to design and synthesize new hybrid nanostructures, which offer great potential for multifunctional devices. Numerous experimental and theoretical investigations have demonstrated the feasibility of single-layered graphene (SLG)-based hybrid structures, such as fullerene–graphene [39], CNT–graphene [40], nanorod–graphene [41] and nanoparticle–graphene [42]. The graphene–fullerene hybrid systems can be potentially used in photovoltaic devices [43], solar cells [44] and Li-ion batteries [45]. The vdW interactions that play a key role in such systems have been studied through experiment or computational approaches in the literature. In this regard, Grimme *et al* [46] used density functional theory (DFT) to determine the noncovalent interactions between graphene sheets and multilayer fullerenes. This theory was also adopted by Laref *et al* [47] to characterize the interactions between C_{60} fullerene and both pristine and defected SLG sheets. Employing the MD simulations, Ma *et al* [48] discovered that the interfacial thermal conductance between C_{60} fullerene and graphene sheet improves by increasing vdW interactions between them. Moreover, Reveles *et al* [49] theoretically calculated that C_{60} fullerene adsorbs on graphene nanoflakes with an energy of 0.76 eV.

From a computational point of view, continuum-based methods outweigh other methodologies proposed for predicting the mechanical properties of nanostructures. Besides being computationally efficient, continuum modelling allows deriving analytical or semi-analytical formulas for the evaluation of vdW interactions. The most widely used method in this area is the continuum approximation, whose validity has been ascertained by atomistic approaches [50]. In this method, nanostructures are approximated as continuous systems with constant atomic densities. This approximation gives rise to evaluate the vdW interactions by means of multiple integrals, which can be performed analytically or numerically [51]. Using the continuum approximation, Ghavanloo and Fazelzadeh [52] modelled the vdW interactions as well as the oscillations of different spherical fullerenes in the vicinity of a fully constrained graphene sheet. Their study revealed that oscillation frequency is highly affected by the size of fullerenes and initial conditions.

This study aims to investigate the oscillations of nested spherical fullerenes (carbon onions) interacting with a SLG sheet. Towards this end, the continuum approximation along with the 6–12 Lennard-Jones (LJ) potential function is employed to model the vdW potential energy and interaction force between the two contacting nanostructures. The equilibrium distance between the carbon onion and the fully constrained graphene sheet is determined through minimization of the total potential energy. Neglecting the frictional effects and also thermally-induced motion of the carbon onion molecule, the equation of motion is directly solved using the fourth-order Runge–Kutta numerical scheme. The conservation of mechanical energy principle is also used to derive a new semi-analytical expression for the precise evaluation of oscillation frequency. Numerical results are presented to study the vdW interactions and dynamic behaviour of carbon onion–SLG sheet oscillators under various system parameters. The results of this research would be of high interest for investigating the adsorption of carbon onion molecules on graphene sheet.

2. VdW potential energy and interaction force

In this section, a continuum-based model is presented to analytically formulate the interactions between a carbon onion molecule and a SLG sheet. Since the electrostatic effect can be ignored [53], this model only considers the vdW interactions arising from the LJ potential function. The geometry of a carbon onion situated above a fully constrained graphene sheet along with the coordinate system is depicted in figure 1. The origin of the Cartesian coordinate system (x, y, z) is assumed to be located at the centre of graphene sheet and the perpendicular distance from graphene sheet to the centre of carbon onion molecule is defined as separation distance which is symbolized by Z. The considered carbon onion, which is made up of N concentric spherical fullerenes, has n carbon atoms in the kth shell as $n(k) = 60k^2$ [54]. Moreover, assuming that carbon atoms are uniformly distributed over the surfaces of the two

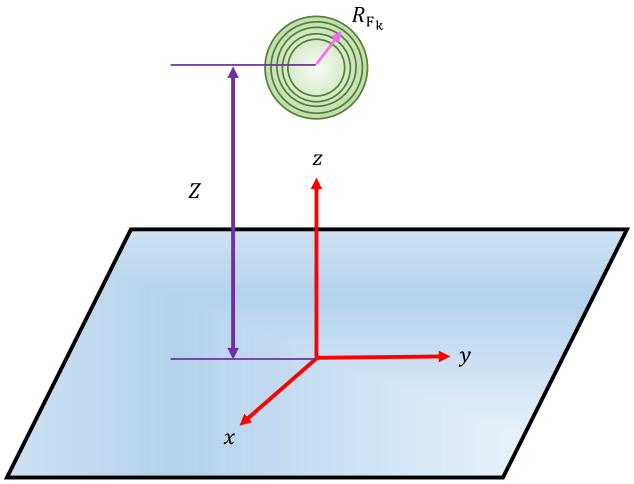

Figure 1. Geometry of carbon onion–SLG sheet oscillators.

molecules, the mean surface density of graphene sheet and the mean surface density of fullerene of radius R_{F_k} are denoted by η_g and η_{F_k}, respectively.

The most straightforward way to determine the vdW interactions between the two contacting nanostructures is the direct method. In this approach, the interactions between each shell of carbon onion and graphene sheet are first calculated and then the total interactions are obtained through summing the interactions between all layers of carbon onion and graphene sheet. Using the continuum approximation in conjunction with the 6–12 LJ potential function, Ghavanloo and Fazelzadeh [52] derived analytical expressions for the evaluation of vdW interactions between a spherical fullerene and a SLG sheet. Rewriting these formulas in the form of sigma notation, we obtain

$$E_k(Z) = \sum_{n=1}^{2} \sum_{m=3n}^{6n-2} \Gamma_{k,n,m} \frac{1}{\left(Z^2 - R_{F_k}^2\right)^{m-1}} \tag{1}$$

$$F_{z_k}(Z) = \sum_{n=1}^{2} \sum_{m=3n}^{6n-2} \lambda_{k,n,m} \frac{Z}{\left(Z^2 - R_{F_k}^2\right)^{m}} \tag{2}$$

in which $E_k(Z)$ is the vdW potential energy between the kth shell of carbon onion and all carbon atoms of graphene sheet and $F_{z_k}(Z)$ is the corresponding interaction force in the z-direction. Note that only the axial interaction force is taken into account due to the symmetric geometry of the considered system.

The parameters introduced in equations (1 and 2) are also given by $\Gamma_{k,n,m} = \frac{\gamma_k C_n G_k^{(m)}}{m-1}$, $\gamma_k = 4\pi^2 R_{F_k}^2 \eta_{F_k} \eta_g$, $\lambda_{k,n,m} = 2(m-1)\Gamma_{k,n,m}$ and

$$\begin{cases} C_1 = -A, & C_2 = \dfrac{B}{5}, & G_k^{(3)} = 1, \\ G_k^{(4)} = 2R_{F_k}^2, & G_k^{(6)} = 5, & G_k^{(7)} = 80R_{F_k}^2, \\ G_k^{(8)} = 336R_{F_k}^4, & G_k^{(9)} = 512R_{F_k}^6, & G_k^{(10)} = 256R_{F_k}^8 \end{cases} \tag{3}$$

Table 1. Numerical values of the constant parameters used in the model [54].

Radius of C_{60}	$R_{F_1} = 3.55$ Å
Radius of C_{240}	$R_{F_2} = 7.12$ Å
Radius of C_{540}	$R_{F_3} = 10.5$ Å
Radius of C_{960}	$R_{F_4} = 13.8$ Å
Radius of C_{1500}	$R_{F_5} = 17.5225$ Å
Mean surface density of C_{60}	$\eta_{F_1} = 0.3789$ Å^{-2}
Mean surface density of C_{240}	$\eta_{F_2} = 0.3767$ Å^{-2}
Mean surface density of C_{540}	$\eta_{F_3} = 0.3898$ Å^{-2}
Mean surface density of C_{960}	$\eta_{F_4} = 0.4011$ Å^{-2}
Mean surface density of C_{1500}	$\eta_{F_5} = 0.3888$ Å^{-2}
Mean surface density of graphene sheet	$\eta_g = 0.3812$ Å^{-2}
Attractive constant	$A = 17.4$ eV Å^6
Repulsive constant	$B = 29 \times 10^3$ eV Å^{12}
Mass of a single carbon atom	$m_0 = 1.993 \times 10^{-26}$ kg

where A and B are attractive and repulsive constants, respectively.

Employing the direct method, the total vdW potential energy and interaction force in the axial direction are respectively calculated from

$$E^{(\mathrm{tot})}(Z) = \sum_{k=1}^{N} E_k \tag{4}$$

$$F_z^{(\mathrm{tot})}(Z) = \sum_{k=1}^{N} F_{z_k} \tag{5}$$

3. Equation of motion and frequency of the oscillation

Knowing the total vdW interaction force and ignoring the frictional force compared to the vdW one [9], the Newton's second law is utilized to write the equation of motion as

$$m_F \frac{\mathrm{d}^2 Z}{\mathrm{d}t^2} = F_z^{(\mathrm{tot})} \tag{6}$$

In equation (6), $m_F = m_0 \sum_{k=1}^{N} n(k)$ represents the total mass of carbon onion molecule, where m_0 is the mass of a single carbon atom. This equation is a second-order nonlinear differential equation from which the oscillation frequency can be obtained numerically. To perform this, the following initial conditions are used:

$$Z(0) = Z_0, \quad \frac{\mathrm{d}Z}{\mathrm{d}t}(0) = V_0, \tag{7}$$

in which Z_0 and V_0 denote the initial separation distance and initial velocity, respectively.

Alternatively, the oscillation frequency of such nano-oscillators can be obtained from the energy equation. This

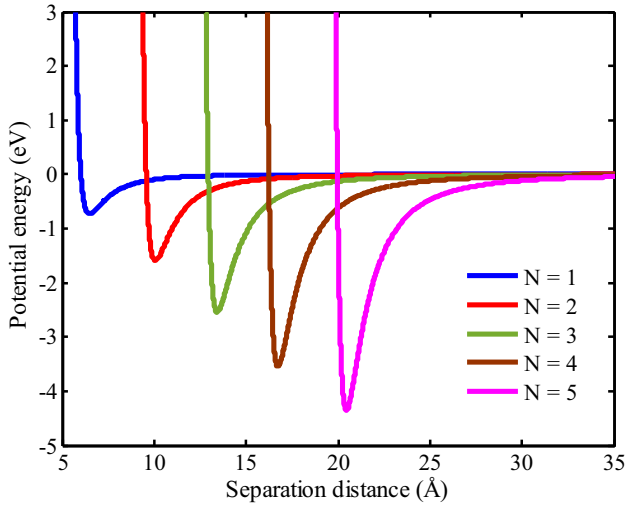

Figure 2. Potential energy profile for different carbon onions interacting with the graphene sheet.

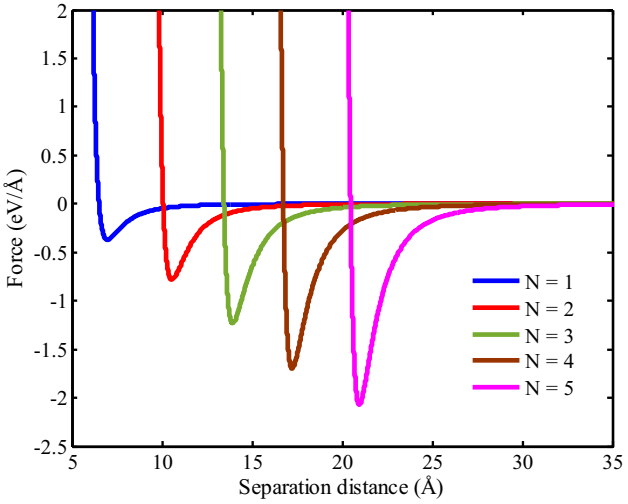

Figure 3. Distribution of vdW interaction force for different carbon onions interacting with the graphene sheet.

equation enables us to derive a semi-analytical expression to precisely estimate the operating frequency. Since the frictional force can be disregarded [9], the total potential energy is conserved. Accordingly, conservation of mechanical energy yields

$$\frac{1}{2}m_F\left(\frac{\mathrm{d}Z}{\mathrm{d}t}\right)^2 + E^{(\mathrm{tot})}(Z) = E^{(\mathrm{tot})}(A_0), \tag{8}$$

where A_0 is the amplitude of motion.

Taking the integral on both sides of the prior equation gives

$$\sqrt{\frac{m_F}{2}}\int_{2Z^*-A_0}^{A_0}\frac{\mathrm{d}Z}{\sqrt{E^{(\mathrm{tot})}(A_0)-E^{(\mathrm{tot})}(Z)}} = \int_0^{\frac{T}{2}}\mathrm{d}t, \tag{9}$$

where Z^* is the equilibrium distance at which total potential energy is minimized and T is the period of motion or the reciprocal of oscillation frequency which is calculated from

$$T = \sqrt{2m_F}\int_{2Z^*-A_0}^{A_0}\frac{\mathrm{d}Z}{\sqrt{E^{(\mathrm{tot})}(A_0)-E^{(\mathrm{tot})}(Z)}} \tag{10}$$

As seen, the integral of equation (10) has singularity at amplitude of motion. In order to numerically evaluate this integral and calculate the period of motion, the singularity must be removed. To perform this, first of all, the period of motion is rewritten as $T = T_1 + T_2$ in which T_1 is a non-singular integral and T_2 is a singular integral defined by

$$T_1 = \sqrt{2m_F}\int_{2Z^*-A_0}^{\delta A_0}\frac{\mathrm{d}Z}{\sqrt{E^{(\mathrm{tot})}(A_0)-E^{(\mathrm{tot})}(Z)}} \tag{11}$$

$$T_2 = \sqrt{2m_F}\int_{\delta A_0}^{A_0}\frac{\mathrm{d}Z}{\sqrt{E^{(\mathrm{tot})}(A_0)-E^{(\mathrm{tot})}(Z)}} \tag{12}$$

where $\delta = 0.99$.

Then, to remove the singularity of equation (12), $E^{(\mathrm{tot})}(A_0) - E^{(\mathrm{tot})}(Z)$ is written as a factor of $(A_0 - Z)$ as follows

$$E^{(\mathrm{tot})}(A_0) - E^{(\mathrm{tot})}(Z) = (A_0 - Z)R(A_0, Z),$$
$$R(A_0, Z)|_{Z=A_0} \neq 0 \tag{13}$$

Using equation (4), one can write

$$E^{(\mathrm{tot})}(A_0) - E^{(\mathrm{tot})}(Z) = \sum_{k=1}^{N}\sum_{n=1}^{2}\sum_{m=3n}^{6n-2}\Gamma_{k,n,m} \times \left(\frac{\left(Z^2 - R_{F_k}^2\right)^{m-1} - \left(A_0^2 - R_{F_k}^2\right)^{m-1}}{\left(A_0^2 - R_{F_k}^2\right)^{m-1}\left(Z^2 - R_{F_k}^2\right)^{m-1}}\right) \tag{14}$$

Table 2. Equilibrium distance and minimum potential energy for different sizes of carbon onion.

N	1	2	3	4	5
Z^* (Å)	6.5093	10.0664	13.4401	16.7361	20.4607
E^* (eV)	–0.7290	–1.5936	–2.5473	–3.5457	–4.3517

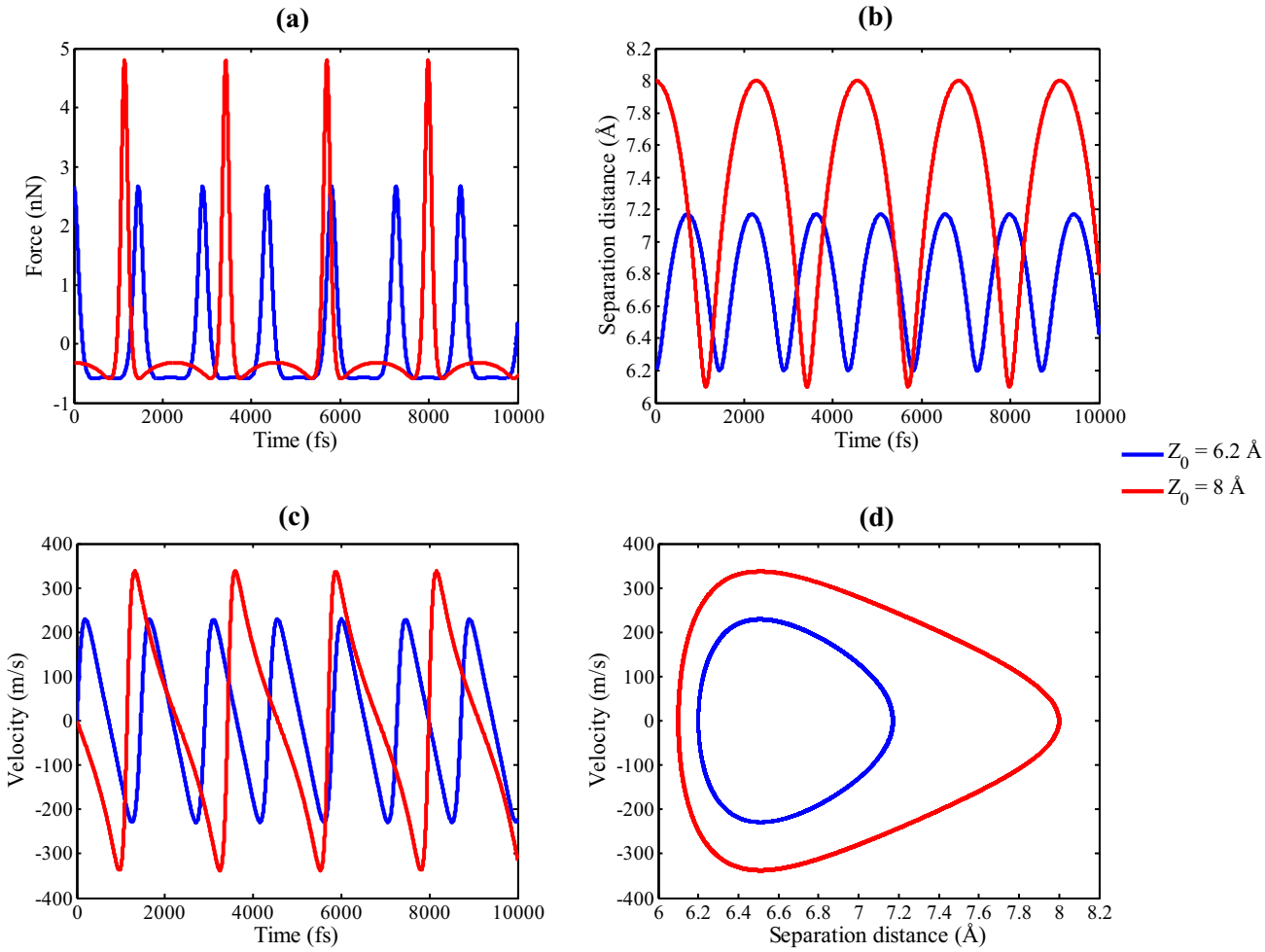

Figure 4. (**a**) Time history of interaction force, (**b**) time history of separation distance, (**c**) time history of velocity and (**d**) phase plot for different initial separation distances reported in [52] ($N = 1, V_0 = 0$).

Applying Khayyam's binomial expansion [55] to the numerator of the preceding equation, then gives

$$\left(Z^2 - R_{F_k}^2\right)^{m-1} - \left(A_0^2 - R_{F_k}^2\right)^{m-1} = \left(Z^2 - A_0^2\right) \sum_{l=1}^{m-1} \left(Z^2 - R_{F_k}^2\right)^{m-l-1} \left(A_0^2 - R_{F_k}^2\right)^{l-1} \quad (15)$$

Substituting equation (15) into equation (14) leads to

$$E^{(\mathrm{tot})}(A_0) - E^{(\mathrm{tot})}(Z) = -(A_0 - Z) \sum_{k=1}^{N} \sum_{n=1}^{2} \sum_{m=3n}^{6n-2} \sum_{l=1}^{m-1} \Gamma_{k,n,m} \times \left(\frac{A_0 + Z}{\left(A_0^2 - R_{F_k}^2\right)^{m-l} \left(Z^2 - R_{F_k}^2\right)^{l}} \right) \quad (16)$$

from which $R(A_0, Z)$ is readily derived as

$$R(A_0, Z) = -\sum_{k=1}^{N} \sum_{n=1}^{2} \sum_{m=3n}^{6n-2} \sum_{l=1}^{m-1} \Gamma_{k,n,m} \times \left(\frac{A_0 + Z}{\left(A_0^2 - R_{F_k}^2\right)^{m-l} \left(Z^2 - R_{F_k}^2\right)^{l}} \right) \quad (17)$$

Eventually, substituting equation (13) into equation (12) and allowing $Z = A_0 \sin^2 \phi$, T_2 becomes

$$T_2 = 2\sqrt{2 m_F A_0} \int_{\sin^{-1}\sqrt{\delta}}^{\pi/2} \frac{\sin\phi \, \mathrm{d}\phi}{\sqrt{R\left(A_0, A_0 \sin^2 \phi\right)}} \quad (18)$$

4. Numerical results and discussion

Using the proposed formulations, numerical results are presented herein for the vdW interactions and oscillation frequency of carbon onion–SLG sheet oscillators. The effects of different system parameters such as size of carbon onion and initial conditions on the dynamic behaviour of such oscillators are fully examined. For the system under consideration, the values of constant parameters required for numerical evaluations are listed in table 1. It should be noted that the radii of C_{60}, C_{240}, C_{540} and C_{960} fullerenes are taken from [56] and the radius of C_{1500} fullerene is taken

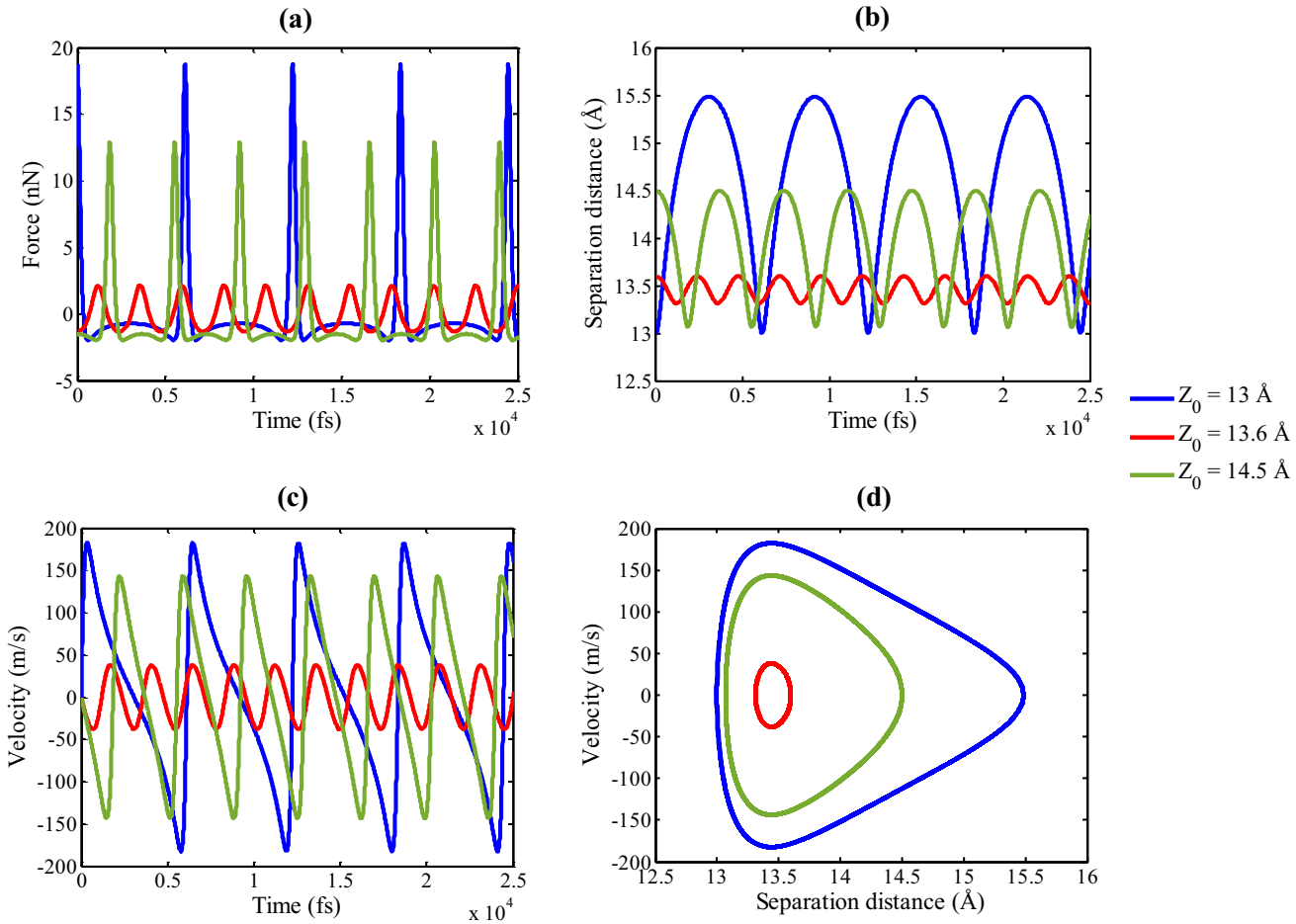

Figure 5. (**a**) Time history of interaction force, (**b**) time history of separation distance, (**c**) time history of velocity and (**d**) phase plot for different initial separation distances $(N = 3, V_0 = 0)$.

from [57]. The mean surface density of fullerene C_n of radius R_F is also calculated from $n/4\pi R_F^2$, where n is the number of carbon atoms in the molecule. In addition, the mean surface density of graphene sheet is equal to that of CNT which is obtained from $4\sqrt{3}/9\sigma^2$, where the carbon–carbon bond length is given by $\sigma = 1.421$ Å [9,52].

The total potential energy *vs.* separation distance is plotted in figure 2 for different sizes of carbon onion. Based on the numerical results, the values of equilibrium distance, Z^*, which minimizes the potential energy along with the minimum potential energy, E^*, are calculated and tabulated in table 2. It can be seen that as the carbon onion gets larger, the equilibrium distance moves further away from the graphene sheet and the magnitude of minimum potential energy increases.

The distribution of vdW interaction force experienced by different nested spherical fullerenes and a SLG sheet is shown in figure 3. Likewise the potential energy profile, the magnitude of minimum interaction force increases by increasing the radius of carbon onion molecule. Based on figures 2 and 3, it can be deduced that vdW interactions vanish for quite large values of separation distances.

In order to perceive the oscillatory behaviour of system in the course of time, the equation of motion is solved here using the fourth-order Runge–Kutta time marching scheme. Considering carbon onion with one layer, the time histories of vdW force, separation distance and velocity along with the phase plot are plotted in figure 4a–d, respectively. These figures are reproduced for the same initial conditions given in the work of Ghavanloo and Fazelzadeh [52]. As expected, our results are entirely consistent with those reported in [52] for C_{60} fullerene–graphene sheet oscillators.

The influence of initial height of carbon onion above the graphene sheet on the time histories of vdW force, separation distance and velocity along with the phase plot is investigated in figure 5a–d, respectively. In this figure, it is assumed that the carbon onion molecule has three shells and is initially at rest. As depicted for all cases, the carbon onion oscillates with respect to the equilibrium distance. The amplitude of motion, velocity and period of motion are also shown to be very sensitive to the initial distance. When the initial height shifts towards the equilibrium distance, the amplitude of motion and the maximum velocity decrease, while the operating frequency increases considerably.

Table 3. Escape velocity for different sizes of carbon onion.

N	1	2	3	4	5
V_{esc} (m s^{-1})	441.9577	292.2279	220.7969	177.9538	145.6013

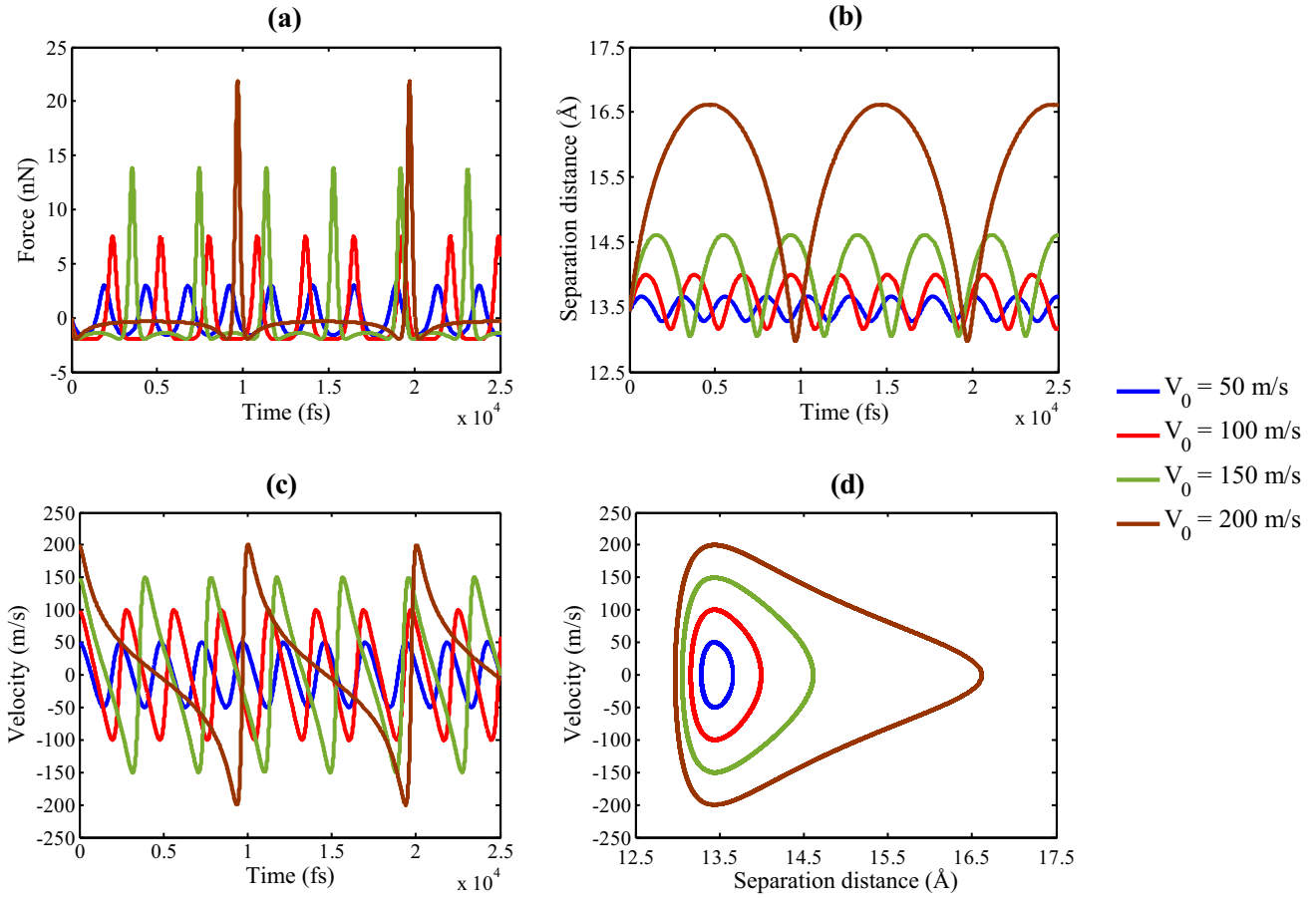

Figure 6. (**a**) Time history of interaction force, (**b**) time history of separation distance, (**c**) time history of velocity and (**d**) phase plot for different initial velocities ($N = 3,\ Z_0 = Z^*$).

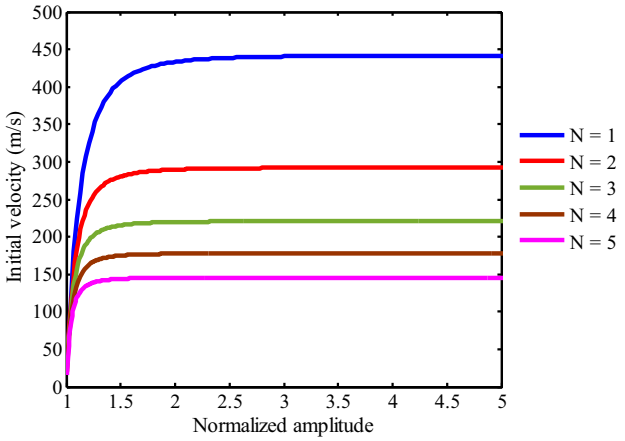

Figure 7. Initial velocity *vs.* normalized amplitude for various carbon onions.

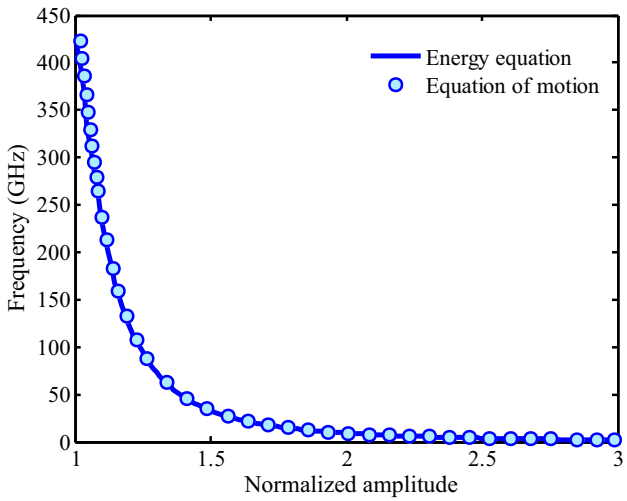

Figure 8. Comparison of oscillation frequency obtained through equation of motion and energy equation ($N = 3$).

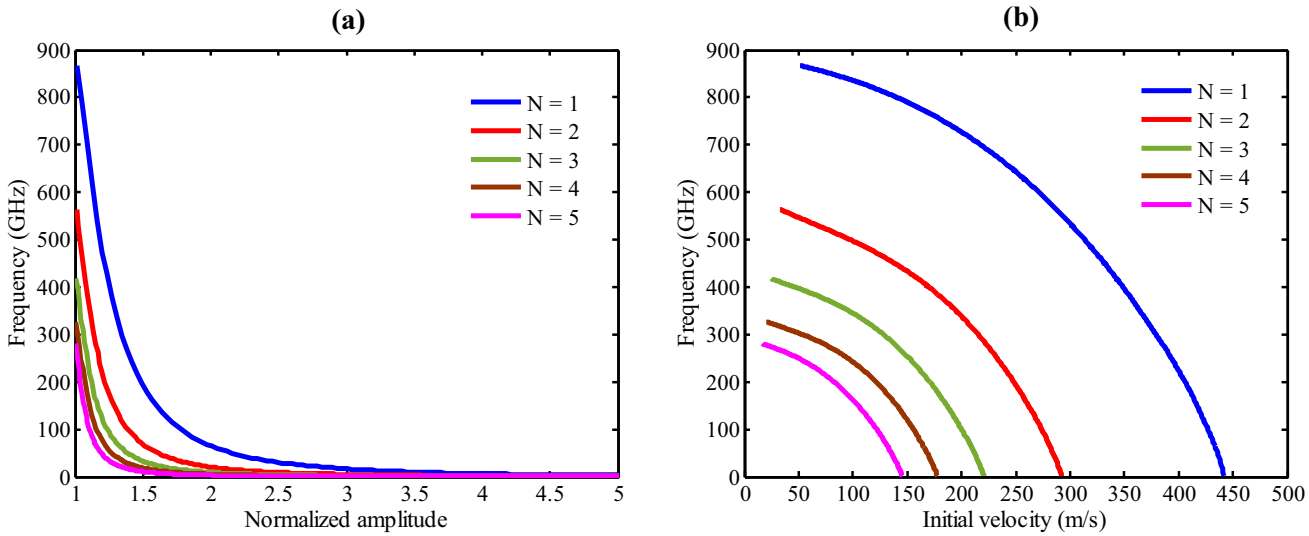

Figure 9. Oscillation frequency *vs.* (**a**) normalized amplitude and (**b**) initial velocity for various carbon onions.

Moreover, it can be observed that the phase plots are not circular. This is ascribed to the quicker growth of velocity compared to the displacement that leads to the egg-shaped curves for all cases.

Considering a carbon onion with three shells, the effect of initial velocity on the time histories of vdW interaction force, separation distance and velocity along with the phase plot is explored in figure 6a–d, respectively. In this figure, it is assumed that the carbon onion is initially located at the equilibrium distance and is trigged with an initial velocity. Likewise figure 5, the amplitude of motion, velocity and period of motion are highly affected by the initial velocity. According to the obtained results, increasing the initial velocity causes both the amplitude of motion and maximum velocity to increase, whereas leads to the reduction of oscillation frequency. For the considered nano-oscillator, a speed limit can be considered above which the carbon onion will no longer oscillates in the vicinity of the graphene sheet. This threshold initial velocity is known as escape velocity and is obtained by

$$V_{\text{esc}} = \sqrt{\frac{-2E^{(\text{tot})}(Z^*)}{m_F}} \tag{19}$$

The values of escape velocity related to several carbon onions are listed in table 3. The results highlight that escape velocity decreases by enlarging the carbon onion molecule. Indeed, as the number of shells rises, the increase in the mass of carbon onion prevails to the increase in the magnitude of potential energy and thus the escape velocity decreases.

Graphically shown in figure 7 is the distribution of initial velocity *vs.* normalized amplitude (the ratio of amplitude to the equilibrium distance) corresponding to several sizes of carbon onion. In this figure, it is assumed that the carbon onion is initially located at the equilibrium distance and is fired with an initial velocity. The ultimate value of this velocity corresponds to escape velocity, which reduces by enlarging the carbon onion molecule. As depicted for all cases, initial velocity quickly reaches a plateau and thus it remains unchanged for a wide range of amplitudes.

Table 4. Maximum frequency for different sizes of carbon onion.

N	1	2	3	4	5
$f_{\max}$(GHz)	867.8	563.9	417.3	326.9	280.4

To compare the frequencies obtained from energy equation and equation of motion, the variation of oscillation frequency with the normalized amplitude is graphically depicted in figure 8. In this figure, the number of shells is taken to be three and it is assumed that the carbon onion is initially separated from the graphene sheet and has no initial velocity. Comparing the obtained results, the accuracy and validity of the proposed oscillation frequency formula is verified. According to the frequency graph, one can observe that frequency behaves decreasingly as the amplitude of motion increases. Hence, the maximum achievable frequency is obtained when the normalized amplitude is almost one.

The influence of size of carbon onion on the variations of oscillation frequency with normalized amplitude and initial velocity is examined in figure 9a and b, respectively. As depicted, the behaviour of frequency with both initial separation distance and initial velocity is decreasing. The values of maximum frequency associated with different carbon onions are listed in table 4. It can be observed that heavier

carbon onion molecules provide lower maximum frequencies.

5. Conclusion

In this study, the dynamic behaviour of nested spherical fullerenes near a fully constrained SLG sheet was investigated. A continuum model based on the continuum approximation and the classical LJ potential function was constructed to calculate the vdW interactions analytically. The equilibrium distance related to this hybrid nanostructure was predicted by minimizing the total potential energy and it was found that this distance comes closer to the graphene sheet as the carbon onion gets smaller. The magnitudes of minimum potential energy and interaction force were also shown to increase by enlarging the carbon onion. Using the actual force distribution, the time histories of separation distance and velocity were obtained through solving the equation of motion numerically. It was observed that amplitude, velocity and period of motion are very sensitive to initial conditions. Moreover, oscillation frequencies were accurately determined using a semi-analytical expression derived from the energy equation. It was demonstrated that the operating frequencies are in the GHz range and may be controlled by the size of carbon onion and initial conditions. Numerical results revealed that smaller carbon onions have higher escape velocities and generate higher frequencies as well. It was further observed that oscillation frequency decreases monotonically as the amplitude of motion or the initial velocity increases.

References

[1] Subramanian A, Dong L X, Nelson B J and Ferreira A 2010 *Appl. Phys. Lett.* **96** 073116
[2] Kang J W, Kim K S, Kwon O K and Lee G Y 2017 *J. Nanosci. Nanotechnol.* **17** 8332
[3] Lin Y W, Jiang W G, Qin Q H and Liao S M 2020 *Physica E* **118** 113943
[4] Chen T, Dumas R K, Eklund A, Muduli P K, Houshang A, Awad A A *et al* 2016 *Proc. IEEE* **104** 1919
[5] Neubrech F, Pucci A, Cornelius T W, Karim S, García-Etxarri A and Aizpurua J 2008 *Phys. Rev. Lett.* **101** 157403
[6] Shan X, Fang Y, Wang S, Guan Y, Chen H Y and Tao N 2014 *Nano Lett.* **14** 4151
[7] Deshpande V V, Chiu H Y, Postma H W C, Mikó C, Forró L and Bockrath M 2006 *Nano Lett.* **6** 1092
[8] Cumings J and Zettl A 2000 *Science* **289** 602
[9] Zheng Q, Liu J Z and Jiang Q 2002 *Phys. Rev. B* **65** 245409
[10] Ma C C, Zhao Y, Yam C Y, Chen G and Jiang Q 2005 *Nanotechnology* **16** 1253
[11] Wong L H, Zhao Y, Chen G and Chwang A T 2006 *Appl. Phys. Lett.* **88** 183107
[12] Legoas S B, Coluci V R, Braga S F, Coura P Z, Dantas S O and Galvão D S 2003 *Phys. Rev. Lett.* **90** 055504
[13] Rivera J L, McCabe C and Cummings P T 2003 *Nano Lett.* **3** 1001
[14] Legoas S B, Coluci V R, Braga S F, Coura P Z, Dantas S O and Galvão D S 2004 *Nanotechnology* **15** S184
[15] Hu W, Song M, Yin T, Wei B and Deng Z 2018 *Nonlinear Dyn.* **91** 767
[16] Guo W, Guo Y, Gao H, Zheng Q and Zhong W 2003 *Phys. Rev. Lett.* **91** 125501
[17] Zhao Y, Ma C C, Chen G and Jiang Q 2003 *Phys. Rev. Lett.* **91** 175504
[18] Liu P, Zhang Y W and Lu C 2005 *J. Appl. Phys.* **97** 094313
[19] Baowan D and Hill J M 2008 *J. Comput. Theor. Nanosci.* **5** 302
[20] Sadeghi F and Ansari R 2017 *Eur. Phys. J. Plus* **132** 309
[21] Ansari R, Sadeghi F and Ajori S 2017 *Eur. J. Mech. A Solids* **62** 67
[22] Ansari R and Sadeghi F 2012 *J. Nanotechnol. Eng. Med.* **3** 011001
[23] Cox B J, Thamwattana N and Hill J M 2008 *Proc. R Soc. A* **464** 691
[24] Kang J W and Lee K W 2014 *J. Korean Phys. Soc.* **65** 185
[25] Zang X, Zhou Q, Chang J, Liu Y and Lin L 2015 *Microelectron. Eng.* **132** 192
[26] Li D and Kaner R B 2008 *Science* **320** 1170
[27] Heyrovska R 2008 *arXiv preprint* arXiv:0804.4086
[28] Booth T J, Blake P, Nair R R, Jiang D, Hill E W, Bangert U *et al* 2008 *Nano Lett.* **8** 2442
[29] Balandin A A, Ghosh S, Bao W, Calizo I, Teweldebrhan D, Miao F *et al* 2008 *Nano Lett.* **8** 902
[30] Cao M, Xiong D B, Yang L, Li S, Xie Y, Guo Q *et al* 2019 *Adv. Funct. Mater.* **29** 1806792
[31] Rahman R, Foster J T and Haque A 2013 *J. Phys. Chem. A* **117** 5344
[32] Tan Q, Kong X, Guan X, Wang C and Xu B 2020 *CrystEng Comm* **22** 320
[33] Liu C, Alwarappan S, Chen Z, Kong X and Li C Z 2010 *Biosens. Bioelectron.* **25** 1829
[34] Xuan Y, Wu Y Q, Shen T, Qi M, Capano M A, Cooper J A *et al* 2008 *Appl. Phys. Lett.* **92** 013101
[35] Qu L, Liu Y, Baek J B and Dai L 2010 *ACS Nano* **4** 1321
[36] Justino C I L, Gomes A R, Freitas A C, Duarte A C and Rocha-Santos T A P 2017 *Trends Anal. Chem.* **91** 53
[37] Tu Z, Wycisk V, Cheng C, Chen W, Adeli M and Haag R 2017 *Nanoscale* **9** 18931
[38] Novoselov K S, Geim A K, Morozov S V, Jiang D, Zhang Y, Dubonos S V *et al* 2004 *Science* **306** 666
[39] Ding X, Chen X, Chen X, Zhao X and Li N 2018 *Sens. Actuators B* **266** 534
[40] Yang Z, Tian J, Yin Z, Cui C, Qian W and Wei F 2019 *Carbon* **141** 467
[41] Hu J, Liu Q, Shi Z, Zhang L and Huang H 2016 *RSC Adv.* **6** 86386
[42] Ayazi H, Akhavan O, Raoufi M, Varshochian R, Motlagh N S H and Atyabi F 2020 *Colloids Surf. B* **186** 110712
[43] Yu D, Park K, Durstock M and Dai L 2011 *J. Phys. Chem. Lett.* **2** 1113
[44] Chakravarty C, Mandal B and Sarkar P 2018 *J. Phys. Chem. C* **122** 15835
[45] Koh W, Lee J H, Lee S G, Choi J I and Jang S S 2015 *RSC Adv.* **5** 32819

[46] Grimme S, Mück-Lichtenfeld C and Antony J 2007 *J. Phys. Chem. C* **111** 11199
[47] Laref S, Asaduzzaman A M, Beck W, Deymier P A, Runge K, Adamowicz L *et al* 2013 *Chem. Phys. Lett.* **582** 115
[48] Ma H, Babaei H and Tian Z 2019 *Carbon* **148** 196
[49] Reveles J U, Karle N N, Baruah T and Zope R R 2016 *J. Phys. Chem. C* **120** 26083
[50] Ansari R, Sadeghi F and Ajori S 2013 *Mech. Res. Commun.* **47** 18
[51] Sadeghi F, Ansari R and Darvizeh M 2016 *Z. Angew. Math. Phys.* **67** 80
[52] Ghavanloo E and Fazelzadeh S A 2017 *Physica B* **504** 47
[53] Baowan D, Peuschel H, Kraegeloh A and Helms V 2013 *J. Mol. Model.* **19** 2459
[54] Thamwattana N and Hill J M 2008 *J. Nanopart. Res.* **10** 665
[55] Shen Y and Cooper G F 2010 *Methods. Inf. Med.* **49** 44
[56] Lu J P and Yang W 1994 *Phys. Rev. B* **49** 11421
[57] Dunlap B I and Zope R R 2006 *Chem. Phys. Lett.* **422** 451